Available online at www.sciencedirect.com

ScienceDirect

Green Energy & Environment xxx (xxxx) xxx

www.keaipublishing.com/gee

Research paper

PVA/PVP blend polymer matrix for hosting carriers in facilitated transport membranes: Synergistic enhancement of CO_2 separation performance

Ragne Marie Lilleby Helberg, Zhongde Dai, Luca Ansaloni, Liyuan Deng*

Department of Chemical Engineering, Norwegian University of Science and Technology, Trondheim, 7491, Norway

Received 31 July 2019; revised 24 September 2019; accepted 13 October 2019
Available online ■ ■ ■

Abstract

CO_2 separation performance in facilitated transport membranes has been reported depended not only on the CO_2 carrier properties but also to a great extent on the polymeric matrix regarding the capacity of retaining water and carriers as well as the processability for coating defect-free ultra-thin films. In this study, the blends of hydrophilic polymers polyvinyl pyrrolidone (PVP) and polyvinyl alcohol (PVA) were studied to find an optimal polymer matrix to host carriers in facilitated transport membranes for enhanced CO_2 separation. It is found out that the optimized blend is 50/50 PVA/PVP by weight, which shows a significant increase in the water uptake (from 63 to 84%) at equilibrium state compared to the neat PVA. Polyethyleneimine (PEI) was employed to provide sample carriers to evaluate the synergistic effect of PVA and PVP on the CO_2 separation performance. A thin film composite (TFC) membrane of the optimized blend (50/50 PVA/PVP with 50 wt% PEI) was fabricated on polysulfone (PSf) porous support. The fabrication of the TFC membranes is simple and low cost, and CO_2 permeance of the optimized blend membrane is nearly doubled with the CO_2/N_2 selectivity remained unchanged, showing great potential for industrial applications of the resulted membranes.

Keywords: TFC membrane; Facilitated transport; CO_2 separation; Polyvinyl alcohol; Polyvinyl pyrrolidone

1. Introduction

The level of CO_2 in the atmosphere has steadily increased during the last decades to up to an alarming level of 400 ppm in 2015 [1]. Several parallel actions have been taken to mitigate CO_2 emission against global warming, including increasing efficiency of current energy sources, the use of renewable energy, and CO_2 capture [2,3].The fifth IPCC assessment report states that the climate goals made by international policymakers are likely not possible without carbon capture and storage (CCS).

Compared to traditional technologies such as physical or chemical absorption and adsorption, gas separation membranes tend to be a cost-effective way of capturing CO_2, due to potentially lower energy consumption and reduced footprint [4,5]. There have been several successful pilot tests of membranes [6]. Most of the current commercial gas separation membranes are polymeric and based on the solution–diffusion mechanism [7] as it is possible to fabricate highly productive polymeric membrane modules at a lower cost, thanks to the flexibility and good processability of polymers. However, there exists a trade-off between permeability and selectivity for most polymeric membranes [8] which limits the application of membranes in many industrial applications, such as CO_2 capture from post-combustion flue gas. Different from most of the polymeric membranes, facilitated transport membranes have the potential to overcome such kind of trade-offs and achieve both high permeability and high selectivity, or at least, to improve the permeability without sacrificing the selectivity, or vice versa [9,10]. In facilitated transport

* Corresponding author.
E-mail address: liyuan.deng@ntnu.no (L. Deng).

https://doi.org/10.1016/j.gee.2019.10.001

membranes, the carriers react with CO_2 and add a chemical contribution to the overall CO_2 transport across the membrane, whereas non-reactive gases such as N_2 will exclusively permeate by the solution–diffusion mechanism, resulting in simultaneously increasing CO_2 permeability and selectivity.

The CO_2 carriers in facilitated transport membranes are usually basic functional groups, which can be free (mobile carriers) or covalently bound to polymeric matrices (fixed-site-carriers). Examples of mobile carriers include ethylene diamine [11], alkanolamines [12] and amino acid salts [13,14]. Polyvinylamine (PVAm) [9,15], polyallylamine (PAAm) [16,17] and polyethyleneimine (PEI) [18] are some of the representative fixed site carriers. Generally, CO_2 facilitated transport agents contain carriers that are either low molecular amines and salts, or highly crystalized polymers; thus a polymer phase is needed to effectively retain these CO_2-carriers and to maintain a reasonable mechanical strength of the membranes in order to ensure the fabrication of gas separation membranes with a defect-free selective layer. So far, polyvinyl alcohol (PVA) [9,19,20] was the most studied and commonly used polymer matrix in this purpose. Cross-linked PVA [21], polyvinyl pyrrolidone (PVP) blended with cross-linked PVA [22], polyethylene glycol (PEG) [23] and Pebax® 1657 [24] were also reported as polymer matrices in CO_2 facilitated transport membranes. PVA is a water-soluble hydrophilic polymer with excellent film forming properties as well as required processability and mechanical strength for membrane fabrication. It is also biodegradable and non-toxic. Deng et al. [9,10] reported PVA in combination with PVAm in order to improve the film formation as well as the mechanical properties of the facilitated transport membranes. Cai et al. [17] reported a PVA/PAAm membrane where PVA was added to reduce the brittleness of PAAm as well as to maintain the hydrophilicity of the facilitated transport membranes. Matsuyama et al. [18] reported a PEI/PVA facilitated transport membrane where the addition of PVA made the carrier retained in the membrane as well as contributing to a high water uptake capacity due to its hydrophilicity. Mondal and Mandal [22] blended chemically cross-linked PVA with PVP in order to increase the thermal stability of the final membrane for high temperature applications before the facilitated transport carriers KOH/PEI was added. Many of the mentioned studies on PVA as a matrix for facilitated transport membranes are based on self-supported films with the thickness of 70–200 μm, where CO_2 permeance is either low or not reported. Additionally, many of the reported results are from gas permeation testing at very low CO_2 partial pressures, where the CO_2/N_2 selectivity is expected to be very high for facilitated transport membranes. It is of interest and great importance to investigate the performance of TFC membranes as it is well known that the performances of membranes with thick films might be very different from those with thin films [21]. Moreover, in order to be used in industry, the membrane materials must be capable of forming thin-films and testing under conditions similar to the real process [25].

Even though most of facilitated transport membrane involves a second polymeric matrix to hold the carriers, there are limited studies dealing with the optimization of the polymer matrix for hosting carriers in facilitated transport membranes. Generally speaking, there are several basic requirements for an ideal "polymer matrix" to serve this purpose, including good film-forming properties and sufficient mechanical strength. The polymer matrix should also be compatible with the CO_2 carriers and able to effectively retain the carriers. In the case of CO_2 capture from flue gas, as water is involved in the CO_2/HCO_3^- reaction cycle for the CO_2 facilitated transport, sufficient water uptake is crucial, and consequently, high hydrophilicity of the polymer matrices is desired. Furthermore, more environment-friendly fabrication processes involving water as the solvent are preferred, excluding the use of more toxic organic solvents typically used for most of the polymeric membranes. Therefore, it is of interest and great importance to develop and optimize the polymeric matrix in a facilitated transport membrane.

This study aims at tailoring a polymeric matrix for CO_2 facilitated transport membranes. Our approach was to optimize the blend of the hydrophilic polymers PVA and PVP. In spite of many advantageous properties as mentioned above, however, PVA is a crystalline polymer, and its high crystallinity hinders the gas permeation in the polymer matrix due to the decreased diffusivity, especially in the dry state. The permeability of PVA can be improved by blending with a less crystalline polymer, such as polyvinyl pyrrolidone (PVP). PVP is an amorphous polymer, which is water soluble and biodegradable [26] with good compatibility with PVA and has good film-forming properties. Besides, PVP is a frequently used hydrophilization agent in water purification and dialysis membranes [27,28] as well as for physically stabilizing suspensions [29]. Based on the preliminary studies in our lab, it was found that blending PVA and PVP takes advantage of the mechanical strength of PVA and the high hydrophilicity of PVP, which increases the capacity of the polymer matrix in retaining water and holding carriers in membranes. However, to the best of our knowledge, no report can be found on the PVP/PVA blend membranes and their influences on the separation performance of the facilitated transport membranes. Thus, in this work, PVP with two different M_w was tested, and the level of PVA/PVP was optimized in the matrix with respect to the water content and CO_2 permeance. After optimizing the level of PVA/PVP, branched polyethyleneimine (PEI) was added into the blend matrix to provide CO_2 carriers for the selective transport of CO_2. PEI was selected for the carriers due to its repeating amine groups, and that it is commercially available at a relatively low cost [30]. The polysulfone (PSf) ultrafiltration membrane was chosen as the support substrate to fabricate the TFC membranes. Various properties of the resultant TFC membranes were studied, including the morphologic (SEM) and gas permeation properties (humid CO_2/N_2 mixed gas permeation test). The material properties of the blend membranes were also studied through the TGA, DSC, FTIR and water uptake tests.

Please cite this article as: R.M. Lilleby Helberg et al., PVA/PVP blend polymer matrix for hosting carriers in facilitated transport membranes: Synergistic enhancement of CO_2 separation performance, Green Energy & Environment, https://doi.org/10.1016/j.gee.2019.10.001

2. Experimental

2.1. Materials

PVA (87–89% hydrolyzed, M_w 85 000–124 000) was purchased from Sigma Aldrich (USA). PVP (M_w 55 000 and M_w 360 000) was supplied by Sigma Aldrich (China), and PEI (M_w 750 000, branched, 50% aqueous solution) by Sigma Aldrich (Germany). PVA, PVP, and PEI were used without further purification. The molecular structure of the polymers is given in Fig. 1.

De-ionized water was used as the solvent for preparing the polymer solutions. Whatman® ReZist® syringe filters (PTFE) were purchased from Sigma–Aldrich (Germany) with a pore size of 5 μm. The flat sheet PSf ultrafiltration (UF) membrane with a molecular weight cut-off (MWCO) of 50 000 Da was purchased from Alfa Laval (Denmark). CO_2/N_2 (10 vol/90 vol) gas mixture and CH_4 (99.999%) used in gas permeation test were supplied by AGA, AS (Norway).

2.2. Membrane preparation

2.2.1. Solution preparation

An aqueous PVA solution (4 wt%) was prepared by adding PVA powder to DI water, followed by heating the solution under stirring at 90 °C for 4 h in a round bottom flask equipped with a condenser. PVP solutions (4 wt%) and PEI solutions (2.5 wt%) were made by mixing the respective polymers and DI water and stirring overnight with a magnetic stirrer at room temperature. The membrane coating solution (2 wt% solid bases) was prepared by mixing the calculated amount of neat PVA, PVP and PEI solution, and diluting with DI water. The solution was ultrasonicated for 2 min (Fisher Scientific™ Model 505 Sonic Dismembrator, 500 W, 20% power level) to remove gas bubbles in the solution. Finally, the solutions were filtered using the Whatman® filter before the membrane preparation.

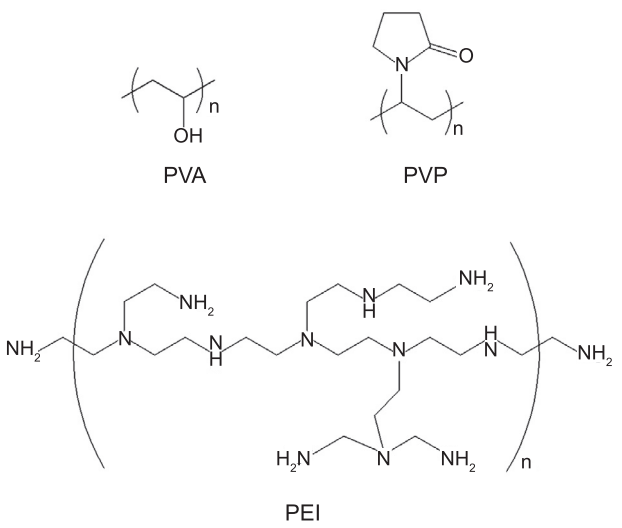

Fig. 1. Chemical structure of PVA, PVP and branched PEI.

2.2.2. Composite membrane preparation

All the composite membranes were prepared using PSf UF membrane as the porous support by a dip coating procedure [19]. Prior to dip coating, the PSf support was loosely attached with aluminum tape to a glass plate and washed in tap water (45–55 °C) for 1.5 h followed by washing with DI water for 30 min. Afterward, the support was sealed with aluminum tape to make sure that no coating solution would penetrate to the backside of the membrane. The support was immersed in the coating solution for 30 s. Then the coated support was kept vertically in ambient condition for 3 h. Afterwards, the PSf support was turned upside down and dip-coated for another 30 s. The composite membranes were kept drying at ambient conditions for approximately 12 h (standing vertically), followed by drying at 45 °C in a convective oven for 3 h to ensure smooth evaporation of water. Finally, the PVA, PVP and PVA/PVP blend membranes were heat-treated at 105 °C for 1 h. PVA/PVP (50:50 wt%) membranes with PEI (25, 50, 75 wt%) were dried in vacuum oven at room temperature for 3 h as PEI will be oxidized at high temperatures.

Self-supported films with thickness of 50–70 μm were also prepared for different physical–chemical characterization. In brief, the self-supported films were prepared by pouring polymer solution into a plastic petri dish and dried at ambient conditions for 5 days. The membrane was further dried in vacuum oven at 45 °C for ~8 h.

2.3. Membrane characterization

The thickness and surface morphology of the composite membranes were investigated using a scanning electron microscope (SEM, Hitachi TM3030, Japan). The membranes were freeze-fractured with liquid nitrogen in order to get an even cross-section. The samples are all coated with gold to make them electrically conductive (Quorum Q150 ES sputter coater, Argon atmosphere, 20 mA for 90 s).

The material properties of the membranes were characterized by TGA, DSC, FT-IR, and water uptake test. The films were kept in a desiccator until the different characterization methods were performed.

The thermal properties of the membrane materials were investigated using TGA (NETZSCH TG 209 Libra F1) and DSC (NETZSCH DSC 214 Polyma). In the TGA test, the samples (~10 mg) were placed in the sample pans and heated from 25 °C to 700 °C with a heating rate of 10 °C min^{-1}. An isothermal step was applied at 105 °C for 20 min in order to ensure complete removal of water in the sample before further heating. Nitrogen was used as both balance gas (flow rate of 10 ml min^{-1}) and sweep gas (flow rate of 60 ml min^{-1}). The TGA results reported here are taken from the heating temperature range from 105 °C to 700 °C. In the DSC test, the sample films (~10 mg) were placed in an aluminum pan. The sample pan, together with an empty reference pan, was heated and cooled in two cycles (10 °C min^{-1} rate) in a nitrogen atmosphere (nitrogen flow rate 40 ml min^{-1}), by first heating from 25 °C to 150 °C and followed by cooling to −50 °C. The

Please cite this article as: R.M. Lilleby Helberg et al., PVA/PVP blend polymer matrix for hosting carriers in facilitated transport membranes: Synergistic enhancement of CO_2 separation performance, Green Energy & Environment, https://doi.org/10.1016/j.gee.2019.10.001

second heating cycle was from −50 °C to 300 °C. The DSC results are taken from the second heating cycle.

FTIR spectroscopy was carried out using a Thermo Scientific Nicolet iS50 FT-IR (ATR mode, wavelength range: 400–4000 cm^{-1}) in order to provide structural insight into the membrane materials. The FTIR spectrum reported here is from the average of 16 scans with a resolution of 4 cm^{-1}. FT-IR was performed on self-supported films at room temperature.

The water uptake of the membrane materials at humid conditions at 23 °C was measured by a gravimetric method. Samples were measured by weighing the sample films before placing them into a desiccator saturated with water vapor and then after every 24 h to determine the water uptake. The percentage of water uptake was calculated using equation (1). The water uptake tests were performed on two replicates of each membrane.

$$\Omega_{\text{water uptake}} = \frac{W_S - W_D}{W_D} \times 100 \quad (1)$$

W_s, and W_D is the weight of the swollen and dry membrane, respectively.

2.4. Humid mixed gas permeation test

The gas separation performance under humid conditions was measured using a constant pressure-variable volume method in a customized mixed gas separation system as shown in Fig. 2 [31]. The steady-state flux of two components in a mixed gas stream of 10% CO_2 and 90% N_2 permeating through a membrane was measured in this test. CH_4 was used as the sweep gas. The relative humidity of the feed gas and the sweep gas was adjusted to 95% for all experiments by two sets of mass flow controllers.

All experiments were carried out at a temperature of 25 °C with a feed pressure of 2 bar and a sweep pressure of 1 bar. The feed flow rate was set to 200 ml min^{-1} and the sweep flow rate 100 ml min^{-1} by two Bronkhorst mass flow controllers. The stage cut was below 0.1% to ensure perfect mixing at both sides of the membranes. The process variables (pressure, temperature, gas flow rate, gas composition, and relative humidity of gases of feed and sweep streams) were continuously monitored, and logged by the LabView Software. The total pressure is regulated by a digital back-pressure regulator from Bronkhorst. The flow rates of both permeate and retentate streams were measured manually by using a bubble flow meter. The feed and sweep gas stream concentrations were analyzed continuously by a Micro GC Agilent 3000. The membrane was placed in a circular stainless steel permeation cell, with an active permeation area of 19.7 cm^2.

In this study, the permeance of CO_2 and N_2 was calculated using a complete mixing model from the total permeance flow as described by equation (2).

$$Q_A = \frac{J_A}{x_{fA}p_f - x_{pA}p_p} \quad (2)$$

where Q_A represents the permeance and J_A is the flux of component A, while x_{fA} and x_{PA} are the mole fraction of A at the feed and permeate sides, respectively. p_f and p_p are the absolute pressure in bar at the feed and permeate sides. In this study, the unit GPU is used to report the gas permeance for a better comparison with the literature values (1 GPU = 10^{-6} cm^3(STP)/cm^2 s^{-1} cmHg = 2.7 × 10^{-3} m^3(STP)/m^{-2} bar h).

The separation factor, $\alpha_{A,B}$, as defined in equation (3) [32], was applied in all mixed gas permeation tests. It is referred to as CO_2/N_2 selectivity throughout the report.

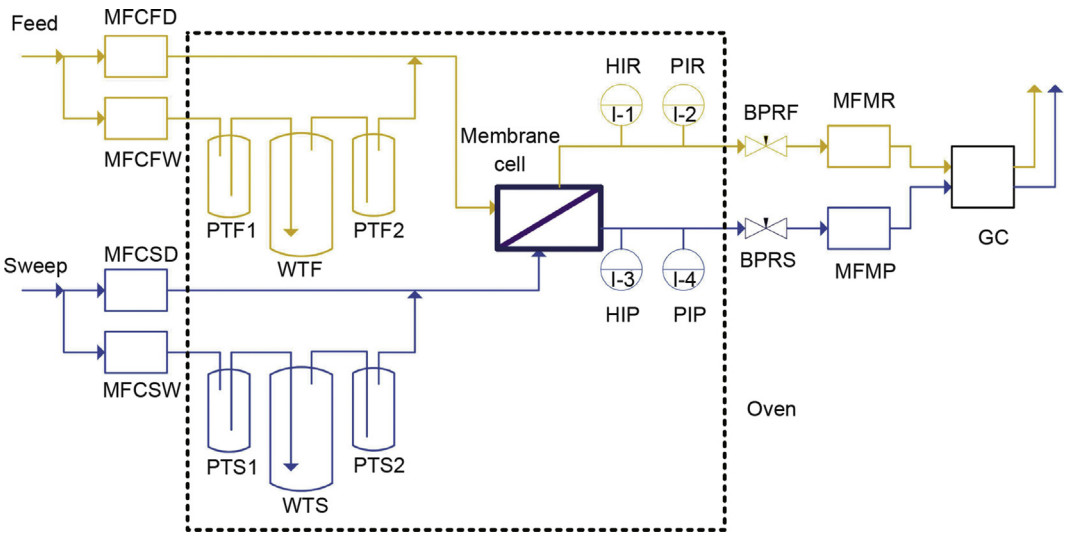

Fig. 2. Mixed gas permeation set up. MFCFD (mass flow controller for feed side, dry gas); MFCFW (mass flow controller for feed side, wet gas); WTF (water tank, feed side); PTF1 and PTF2 (protective tanks, feed side); HIR and PIR (Humidity and pressure indicator, retentate side); BPRF (back pressure regulator, feed side); MFMR (mass flow meter, retentate side); MFCSD (mass flow controller sweep side, dry gas); MFCSW (mass flow controller sweep side, wet gas). WTS (water tank, sweep side); PTS1 and PTS2 (protective tanks, sweep side); HIP and PIP (humidity and pressure indicator, permeate side); BPRS (back pressure regulator, sweep side); MFMP (mass flow meter, permeate side); GC (gas chromatograph). Reproduced with permission from Ref. [31].

Please cite this article as: R.M. Lilleby Helberg et al., PVA/PVP blend polymer matrix for hosting carriers in facilitated transport membranes: Synergistic enhancement of CO_2 separation performance, Green Energy & Environment, https://doi.org/10.1016/j.gee.2019.10.001

$$\alpha_{A,B} = \frac{y_A^p}{y_B^p} \Big/ \frac{y_A^f}{y_B^f} \quad (3)$$

where y_A^p and y_B^p are the molar fractions of A and B at the permeate side and y_A^f and y_A^f are the molar fractions of A and B at the feed side, respectively. The gas permeation data are calculated by an average of minimum of 2 h measurement after steady-state is reached. A minimum of two membranes are tested each time.

3. Results and discussion

3.1. Optimization of PVA/PVP blend

PVA has been reported as a common polymer matrix to host carriers for facilitated transport membranes [9,14,19,33], but PVA membranes suffer from low gas permeance due to its crystalline nature. PVP was proposed to blend with PVA in order to reduce the crystallinity so as to increase the permeability. The water uptake of the final matrix should also increase as PVP is more hydrophilic. These two hydrophilic polymers were hence blended and the properties of different combinations of the two polymers were studied to find the optimum blend for the best host matrix for facilitated transport carriers. To optimize the level of PVA and PVP, the membranes of following materials, namely neat PVA, neat PVP and the various PVA/PVP blends (25/75, 50/50 and 25/75 w/w), were prepared and characterized by various techniques, as shown in Figs. 3 and 4. All mentioned compositions here are in wt%. It is worth mentioning that two molecular weights of PVP were tested initially (M_w 55 000 and M_w 360 000), but the surfaces of the membrane made from the 55 000 M_w PVP were covered with cracks and the films were too brittle to be further tested. Hence, the 55 000 M_w PVP was excluded and only the mechanically robust 360 000 M_w PVP was used in this study.

The membrane morphology of the PVA/PVP (50/50) TFC membrane is shown in Fig. 3a (cross-section) and 3b (surface). Neat PVA, neat PVP, as well as the PVA/PVP blend membranes of other ratios, were also studied using SEM and results can be found in Supporting information Figs. S1 and S2. All the prepared membrane surfaces were smooth without noticeable defects. It is found out that the neat PVA and PVA/PVP blend membranes show an average thickness in the range of 0.4–0.8 μm (both before and after gas permeation testing), where no visual differences of the surfaces of the membranes with different compositions can be found.

Neat PVP has an average thickness of 793 nm. However, the morphology of the neat PVP membrane seems different from the other samples; the thickness of the membrane is varying to a greater extent for the tested membranes, as demonstrated by a significant higher standard deviation of thickness (shown in Supporting information Fig. S2 and Table S1). A possible explanation for this phenomenon might be that PVP was partially solvated by the absorbed water vapor from the gaseous stream during the gas permeation test undergoing significant relaxations of the polymeric matrix. The hydrophilic character of PVP is further discussed in the water uptake section. The average selective layer thicknesses haves been summarized and presented in Table S1 in Supporting information.

Fig. 3c shows the FT-IR spectra of the neat PVA, neat PVP and PVA/PVP blend films. The detailed peak assignment report is given in Table 1. For neat PVA as well as PVA/PVP blends, the big broad peak at 3290 cm^{-1} to 3446 cm^{-1} represents the O–H vibrations. The broad width of the peaks shows that the O–H groups are hydrogen bonded. Although all samples were dried before the tests, some samples might have still absorbed water from the surroundings, which could affect the peak intensity.

Ping et al. examined the shift in frequencies of the groups involved in interactions between PVA and PVP [34], namely the carbonyl group of PVP, C–O of PVA, and O–H of PVA. Similar shifts in frequencies are observed in our work as shown in Table 2; the carbonyl stretching frequency of PVP is decreasing with the increasing amount of PVP and the C–O stretching frequency, as well as the O–H stretching frequency of PVA, is increasing with the increasing amount of PVP. According to the FTIR spectra and the description given by Ping et al. [34] about the hydrogen bonding interactions in PVA/PVP blends, the hydrogen bonding between O–H in PVA is reduced when adding PVP to PVA (the O–H and C═O bonding increases), leading to the reduction of PVA crystallization, especially when increasing PVP content to 50% and beyond.

TGA results of the PVA/PVP samples prepared in the study are shown in Fig. 3d. As mentioned in the experimental section, in the TGA test, the sample was heated at 105 °C for 20 min to remove the absorbed moisture in the samples. The thermal stability of the films is evaluated and compared using the onset decomposition temperature (T_{onset}) values read from the graph. T_{onset} is defined as the intersection between the initial weight curve and tangent of the decomposition curve. It is a clear trend that the addition of PVP increases the thermal stability of the blend. Neat PVA shows a T_{onset} of around 290 °C, while adding PVP gradually shifts the T_{onset} up to about 410 °C for neat PVP. The 50 PVA/50 PVP blend has a T_{onset} of around 300 °C. The T_{onset} values for PVA and PVP obtained in this work are in accordance with literature values for both PVA [22] and PVP [35]. All the samples satisfy the requirements for post-combustion CO_2 capture, which typically operates at temperatures below 80 °C. As observed from the curves, the samples containing PVA shows a two-step decomposition. The first main weight loss region was due to the loss of hydroxyl groups. The second weight loss region (400 °C–500 °C) is most likely due to the decomposition of the polymer backbone. The total percentage of weight loss is approximately the same for all films.

Fig. 3e presents the results from the DSC analysis in the temperature range −15 °C to 150 °C. Neat PVA shows a glass transition temperature of 47 °C. Cassu and Felisbert [36] reported a T_g of 59 °C for a similar PVA grade (87.7% hydrolyzed, M_w 127 000 g mol^{-1}). The difference may be attributed

Please cite this article as: R.M. Lilleby Helberg et al., PVA/PVP blend polymer matrix for hosting carriers in facilitated transport membranes: Synergistic enhancement of CO_2 separation performance, Green Energy & Environment, https://doi.org/10.1016/j.gee.2019.10.001

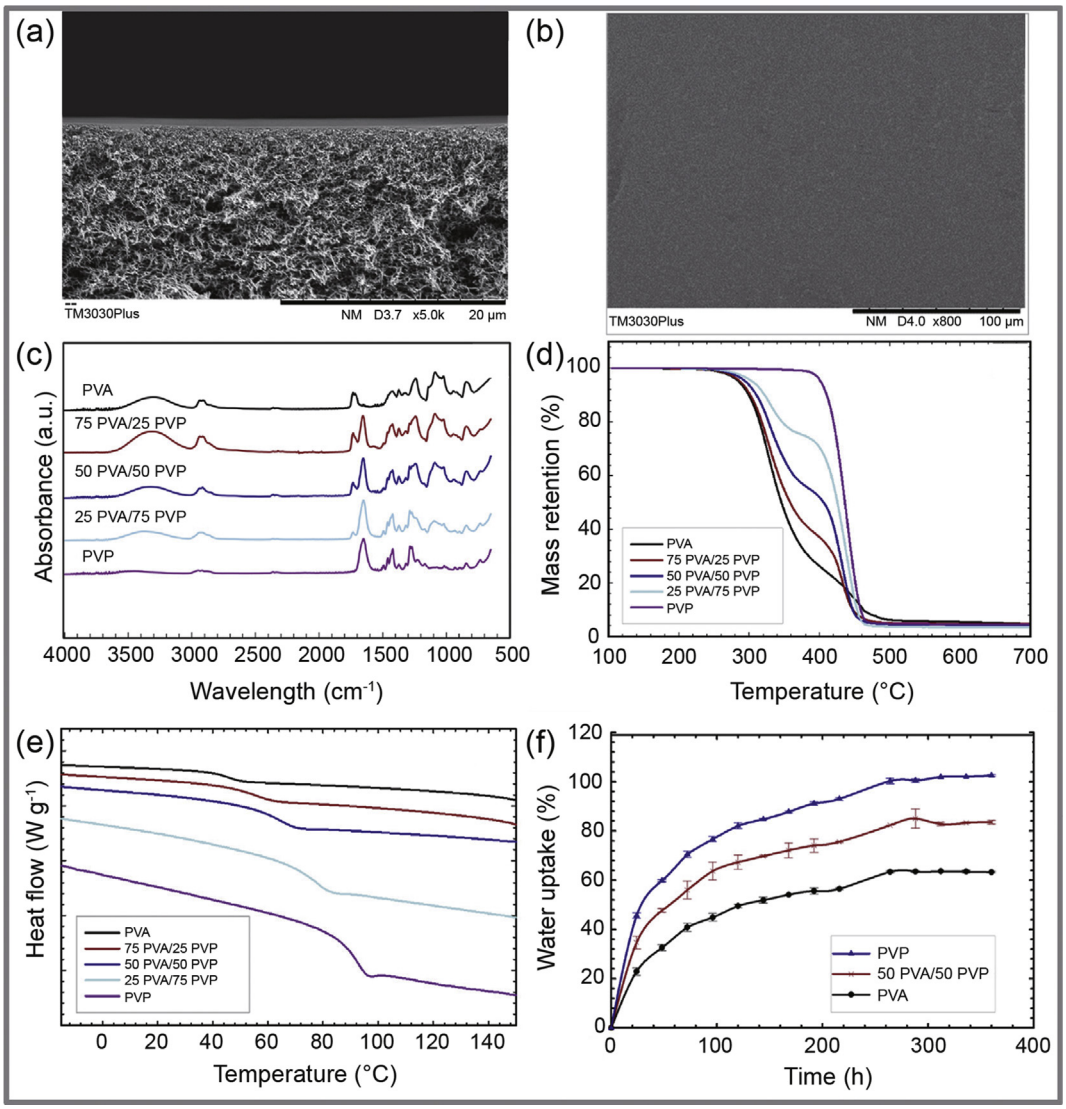

Fig. 3. Characterization of PVA/PVP blends: a) SEM image cross-section 50 PVA/50 PVP TFC membrane, b) SEM image surface 50 PVA/50 PVP TFC membrane, c) FT-IR spectra, d) TGA graph, e) DSC analysis, and f) Water uptake.

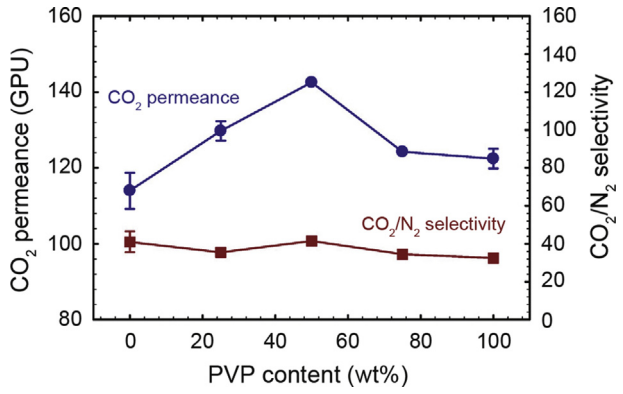

Fig. 4. Effect of increasing PVP content to PVA on CO_2 permeance and CO_2/N_2 selectivity.

Table 1
FT-IR peak assignments [34].

Wavenumber (cm^{-1})	Peak assignment
3290–3446	O–H and N–H stretching
2910–2919	$(C–H)_n$ stretching
1733	C=O stretching of ketone[a]
1659–1652	C=O stretching of lactam (amide II band)
1419–1421	CH_2 bending
1373	C–H deformation
1240–1285.2	C–O stretching ether linkage, C–N stretch PVP
1067–1095	C–O stretching primary alcohol
843	O–H out of plane bending

[a] PVA used in this study has a hydrolysis degree of 87–89%, hence about 11–13% acetate groups are present in the polymer structure.

to a slightly lower M_w of PVA used in this study. By increasing the PVP content, the T_g showed a monotonic increase from 47 °C to 97 °C. Several literature values of T_g for PVP can be found, ranging from 54 °C to 175 °C [37], depending on factors such as polymerization process, molecular weight, amount of absorbed water in the material and pre-treatment of

Please cite this article as: R.M. Lilleby Helberg et al., PVA/PVP blend polymer matrix for hosting carriers in facilitated transport membranes: Synergistic enhancement of CO_2 separation performance, Green Energy & Environment, https://doi.org/10.1016/j.gee.2019.10.001

Table 2
Wavenumber of the C═O, C−O and O−H groups as a function of PVP content in PVA.

PVP content (wt%)	Wavenumber C═O (cm^{-1})	Wavenumber C−O (cm^{-1})	Wavenumber O−H (cm^{-1})
0	–	1067	3290
25	1659	1089	3307
50	1651.84	1092	3355
75	1651.82	1095	3374

the sample prior to testing [38]. The presence of one single T_g for the blends indicates that the blend is homogeneous and PVA and PVP are fully miscible.

Based on the preliminary study, the water uptake of the PVA/PVP blend is nearly proportional to the PVP content in the PVA/PVP blends. Even though the samples with higher PVP content (i.e., neat PVP and PVA/PVP of 25/75) exhibit higher water uptake, the blend membrane of PVA/PVP (50/50) has the best film based on the observation. The neat PVP has a very poor film integrity, which was observed from visual inspection of the films during the water uptake testing where the resultant PVP film under humid conditions appeared to be gel-like, not a film. A poor film integrity is negative for the separation performance as it gives a big error in the selective layer thickness of the thin film composite membranes (see Fig. S2 and Table S1 in the Supporting Information). Therefore, the water update of the PVA/PVP (50/50) blend was further studied, the comparison of which with those of the neat PVA and PVP samples are presented in Fig. 3f. Results from Fig. 3f show that neat PVP has a higher equilibrium water uptake (103%) than neat PVA (63%). The PVA/PVP (50/50) blend has an equilibrium water uptake of 84%. In a study by Deng and Hägg, a water uptake of 75% was obtained for PVA [39], but the PVA grade used in their study has a higher hydrolysis degree as well as lower molecular weight, which are both factors that might increase the water uptake. According to the visual inspection during the water uptake testing, the resultant PVP film under humid conditions appeared to be gel-like, while the PVA film, as well as the PVA/PVP (50/50) blend sample, were still solid. In addition, the dry PVP film is more brittle than that of PVA; the blend of PVP with PVA has resulted in both better film forming and mechanical properties.

The separation performance of the PVA/PVP (50/50) blend membrane is also improved, as presented in Fig. 4. The membrane of the PVA/PVP (50/50) blend shows the highest CO_2 permeance. The neat PVA membrane shows the CO_2 permeance of 114 GPU, comparable to the value reported by Saeed and Deng [40] (CO_2 permeance of 110 GPU and a CO_2/N_2 selectivity of 60 ± 5) tested at 2 bar. As the PVP content in the PVA/PVP blends increases, the CO_2 permeance shows an optimum value of 143 GPU at PVA/PVP (50/50) composition. The membranes of PVA/PVP (75/25) and PVA/PVP (25/75) have similar CO_2 permeance as those of the neat PVA and PVP. Although PVP is more hydrophilic than both PVA and the 50/50 PVA/PVP blend while PVA has the best membrane coating, the blend membrane of PVA/PVP (50/50) has the highest CO_2 permeance among the tested membranes, demonstrating the synergetic enhancement of the two polymers in the blend membrane.

It is also observed that the addition of PVP could reduce the crystallinity of PVA, as suggested by Zhang et al. [41], where the crystalline phase of PVA disappeared at a PVA level below 46% in a PVA/PVP blend. The reduced crystallinity is beneficial for a relatively higher CO_2 permeance. This effect is also supported by the FT-IR results as discussed above. In addition, when considering the mechanical properties and water uptake, the 50/50 blend is also shown combined the advantage of both PVA and PVP. The blend membrane of PVA/PVP (50/50) was thus selected for further investigation.

The effects of the blend composition on the CO_2/N_2 selectivity is also shown in Fig. 4. Compared to the CO_2 permeance, the CO_2/N_2 selectivity is only moderately reduced as the PVP content increases from 0 to 100 wt%.

3.2. Effect of PEI as CO_2 carriers in the optimized PVA/PVP matrix

It is of interest to investigate whether the optimized PVA/PVP blend can serve as a matrix for facilitated transport carriers and to increase the final performance of the membrane. PEI was employed as an additive to provide sample facilitated transport carriers in this work. The PVA/PVP (50/50) blend membranes with the addition of PEI at different content were prepared and characterized, as shown in Figs. 5 and 6.

The morphology of the membranes was studied using SEM and the results are presented in Fig. 5a, which shows the cross-section of the membrane with 50% PEI. This sample, as well as the membranes containing 25 and 75 wt% PEI, showed a smooth coating of the defect-free selective layer with the thicknesses in the range of 550 nm−890 nm (SEM image shown in Supporting information Fig. S3, average selective layer thicknesses in Table S2). Membranes made of 25% PEI and 50% PEI have the thicknesses in the same range (550−600 nm), and with increasing PEI content, the membrane became slightly thicker (~890 nm for the membrane with 75% PEI). A neat PEI TFC membrane of thickness 319 nm was also obtained, but it was visually observed that the PEI can be gradually dissolved in water at room temperature and the coating layer of this membrane was fragile and brittle at dry state. The addition of a second polymer phase (e.g., PVA) is clearly needed to achieve a suitable selective layer in order to effectively contain the CO_2 carriers from PEI. Please note that the coating solution concentrations of all above membranes are the same (2.0 wt% of polymers in total) as indicated in the experimental section. The thicknesses of the coating layers vary significantly in the membranes of different PEI ratios, which is believed mainly due to the viscosity differences in the coating solutions; similar phenomenon has been widely reported [42]. All the prepared membrane surfaces were smooth without noticeable defects and without differences between the different compositions.

FTIR tests were also carried out and the results are shown in Fig. 5b. The peak around 3200 cm^{-1} to 3400 cm^{-1} for the PVA/PVP blend as well as films with PEI represents the O−H

Please cite this article as: R.M. Lilleby Helberg et al., PVA/PVP blend polymer matrix for hosting carriers in facilitated transport membranes: Synergistic enhancement of CO_2 separation performance, Green Energy & Environment, https://doi.org/10.1016/j.gee.2019.10.001

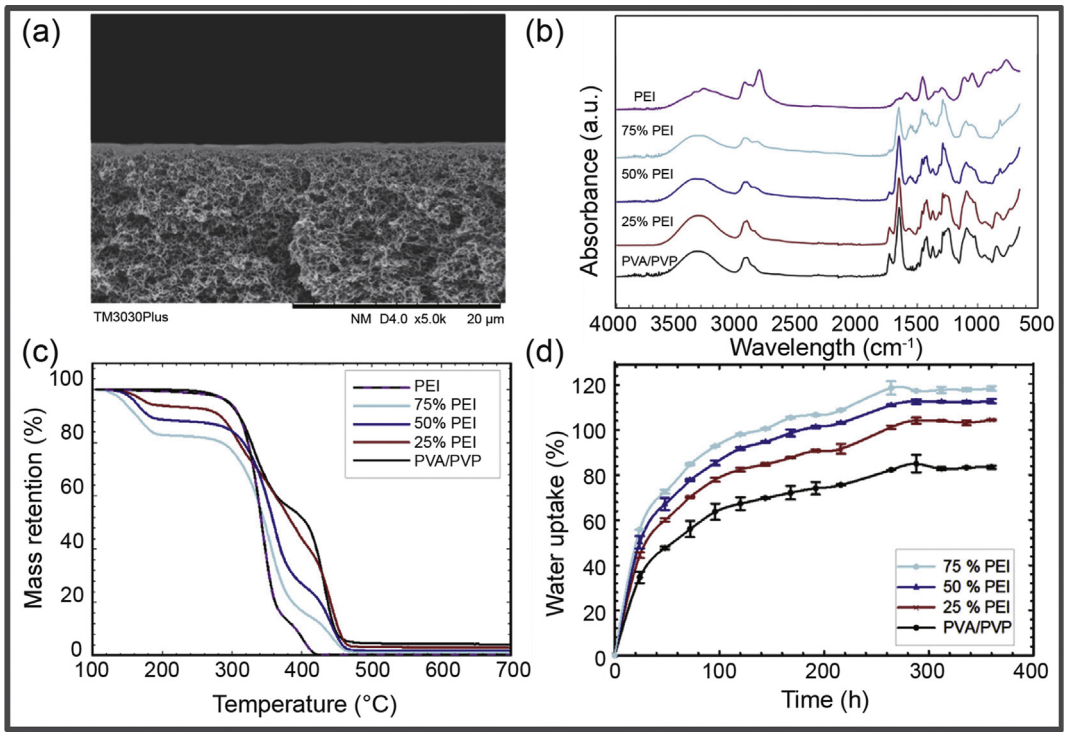

Fig. 5. Characterization of membranes containing different amounts of PEI added to 50/50 (wt%/wt%) PVA/PVP blend: a) SEM images, b) FT-IR spectra, c) TGA graph and d) Water uptake.

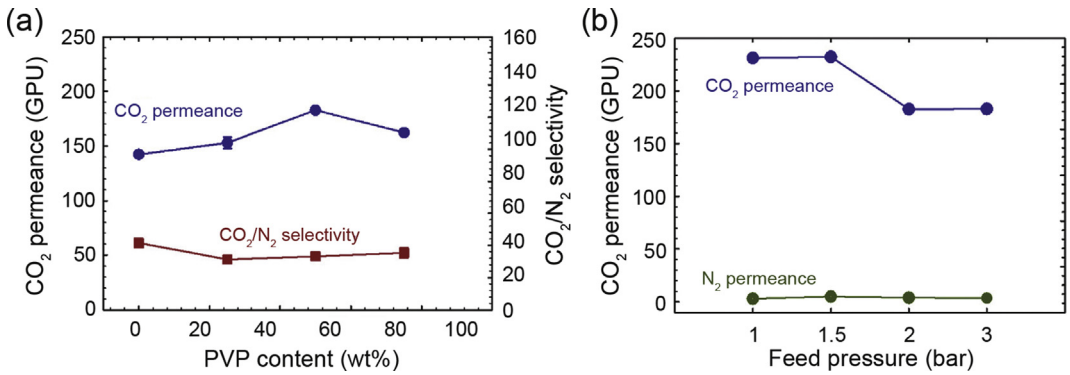

Fig. 6. Effect of a) increasing PEI content in a PVA/PVP blend on CO_2 permeance and CO_2/N_2 selectivity and b) Effect of feed pressure on gas separation performance of the membrane with 50 wt% PEI.

stretching vibrations [43]. The N–H stretching of amines appears in the same region as O–H stretching of alcohols, which are usually weaker but sharper peaks. For neat PEI, the peak at 1594 cm^{-1} represents the N–H bending vibration of primary amines of PEI [44]. For the PEI/PVA/PVP blends, this peak is shifted towards slightly lower wavenumber (1559 cm^{-1}) due to the polyion formation when PVA is blended with PEI [45]. Usually, secondary amines do not show bands within this region.

Results from the TGA test (Fig. 5c) show that the T_{onset} decreases significantly when PEI is added to the PVA/PVP (50/50) blend. Both neat PVA/PVP and neat PEI have relatively high T_{onset} values (300 °C and 325 °C, respectively). Shen et al. also reported the T_{onset} of about 325 °C for neat PEI [46]. However, in this study, the T_{onset} decreases to 160 °C, 150 °C and 140 °C for films containing 25% PEI, 50% PEI and 75% PEI, respectively. The similar trend was also observed by Rao et al., where a PVA/PEI blend showed a lower T_{onset} as compared to neat PVA [45]. The drop in thermal stability is most likely related to the ionic interactions taking place between PVA/PVP and PEI molecules [45]. However, despite the lower T_{onset} of the PEI/PVA/PVP blends, all the samples are stable at the operating temperature for post-combustion CO_2 capture, which is typically below 80 °C.

Results from the water uptake tests (Fig. 5d) show that the water uptake increases significantly with the PEI content: the equilibrium water uptake of 50% PEI is 120% while it is 84% for the neat PVA/PVP (50/50) blend. By visually inspecting

Please cite this article as: R.M. Lilleby Helberg et al., PVA/PVP blend polymer matrix for hosting carriers in facilitated transport membranes: Synergistic enhancement of CO_2 separation performance, Green Energy & Environment, https://doi.org/10.1016/j.gee.2019.10.001

Table 3
Comparison of separation performance of similar membranes reported in the literature.

Membrane material	CO_2 permeance (GPU)	CO_2/N_2 selectivity	Thickness[a]	CO_2 partial pressure	Ref.
PEI/PVA/PEG	–	25	NA (SSM)	1	[47]
PEI/PVA	2.2	60	220 μm (SSM)	0.2	[18]
PEI/PVA	85	NA	10 μm (SSM)	0.2	[18]
PEI/PVA/PES	89	35	2 μm (TFC)	0.002–0.004	[48]
PEI/PVA/PVP	183	35	550 nm (TFC)	0.2	This study

[a] SSM = self supported membranes, TFC = thin film composite membrane.

the films exposed in a fully humidified environment, it is clear that the 75% PEI in PVA/PVP film appears to be gel-like, while the other blends are still in a film-form. It is well accepted that for hydrophilic membranes a higher water uptake will result in an increase of CO_2 permeance, but in order to obtain good performance, there must be a balance between high water uptake and a proper film formation/mechanical film integrity.

Mixed gas permeation tests were also carried out for the PEI/PVA/PVP membranes. As it can be seen from Fig. 6a, the CO_2 permeance significantly increases along with the PEI content to up to 50 wt% starting from the neat PVA/PVP (50/50) blend membrane; the CO_2 permeance increases from 143 GPU to 183 GPU. Further increasing the PEI content to 75 wt% in the membranes decreases the CO_2 permeance, hence the optimum PEI level was found to be 50 wt%. The neat PEI membrane has poor mechanical properties and consequently a low and unstable separation performance, indicating that a polymer matrix is needed to hold the carriers in the TFC membranes. Fig. 6a also presents the CO_2/N_2 selectivity of the membranes with various PEI contents. As shown in the figure, the CO_2/N_2 selectivity is firstly decreasing when adding PEI to neat PVA/PVP, followed by a small increase with increasing PEI content from 50 wt% to up to 75 wt%. Nevertheless, the overall changes in the CO_2/N_2 selectivity is not significant (±10%); thus, the optimization of the membranes is mainly regarding the CO_2 permeance.

As the membrane with 50 wt% PEI showed the highest CO_2 permeance among the tested membranes, it was selected to study the effect of feed pressure on the separation performances, as shown in Fig. 6b. With the total feed pressure increasing from 1.5 to 3 bar, a significant reduction can be found in the CO_2 permeance, which is a typical trend in facilitated transport membranes, and this phenomenon is normally referred to as “carriers saturation”. On the other hand, the effect of feed pressure on the N_2 permeability is limited in the tested pressure range.

Table 3 summarizes the results of PEI-based membranes reported in the literature. It is worth mentioning that the chosen literature data are only those tested at similar operating conditions (~25 °C, humid conditions, 1–2 bar feed pressure, CO_2 partial pressure of 0.1–0.2 bar), as the total feed pressure and the CO_2 partial pressure have a significant impact on the performance of facilitated transport membranes. Moreover, according to the literature, the similar facilitated transport membranes exhibited better performance at higher temperatures. For example, Mondal and Mandal [22] reported a CO_2/N_2 selectivity of 202 from a similar membrane, a self-supported PEI/cross-linked PVA/PVP/KOH membrane of thickness 69 μm, when the membrane was tested at elevated temperatures (90–125 °C). As discussed in the Introduction and shown in Table 3, most of the relevant literature of PEI-based membranes reported only self-supported membranes. Limited studies can be found in literature that are directly comparable to the results obtained in this study. Nevertheless, it is important to investigate the performance of thin film composite membranes as it is well known that the performance of thick film membranes might be very different from that of the thin films. For practical application, membrane materials must be able to form thin-films and operate at relevant industrial conditions [33].

4. Conclusion

An improved polymeric matrix for facilitated transport carriers was developed and optimized regarding the capacity of retaining water and carriers and the processability for coating defect-free ultra-thin films. A 50/50 PVA/PVP blend showed a synergetic effect with a significant improvement in CO_2 permeance and water uptake with a similar CO_2/N_2 selectivity as neat PVA membranes as well as the membranes of other blends. It was further demonstrated that the optimized PVA/PVP blend can serve as a matrix for facilitated transport carriers and the addition of 50% PEI increased the CO_2 permeance due to the facilitated transport effect of the amine-based carriers. The membranes were fabricated as TFC membranes with PSf ultrafiltration membrane as the porous substrate. The membranes were characterized and evaluated under typical post-combustion CO_2 capture conditions. A considerably higher CO_2 permeance than similar membranes reported in the literature was documented. In addition, the equilibrium water uptake after exposure to saturated water vapor was reported increased significantly from 63 ± 0.3% (neat PVA) to 118 ± 1% (optimized PEI/PVA/PVP blend).

The obtained PVA/PVP blend is considered to be a promising matrix to host facilitated transport carriers to further improve the CO_2 permeance. Moreover, both PVA and PVP are non-toxic and commercially available at a low cost. The

Please cite this article as: R.M. Lilleby Helberg et al., PVA/PVP blend polymer matrix for hosting carriers in facilitated transport membranes: Synergistic enhancement of CO_2 separation performance, Green Energy & Environment, https://doi.org/10.1016/j.gee.2019.10.001

preparation method is simple and membranes can easily be reproduced. In the future work, PVA/PVP blend membranes containing different types and amounts of carriers may be studied to further optimize the membrane and improve the separation performance. The potential of the PVA/PVP blend matrix to hold compatible nanoparticles may also be explored.

Conflict of interest

The authors declare that there is no conflict of interest regarding the publication of this article.

Acknowledgment

The authors would like to acknowledge the Norwegian Research Council for the financial support to this work through the Nano2021 program (project number 239172).

Appendix A. Supplementary data

Supplementary data to this article can be found online at https://doi.org/10.1016/j.gee.2019.10.001.

References

[1] T.P. Senftle, E.A. Carter, Acc. Chem. Res. 50 (2017) 472–475.
[2] M. Bui, C.S. Adjiman, A. Bardow, E.J. Anthony, A. Boston, S. Brown, P.S. Fennell, S. Fuss, A. Galindo, L.A. Hackett, J.P. Hallett, H.J. Herzog, G. Jackson, J. Kemper, S. Krevor, G.C. Maitland, M. Matuszewski, I.S. Metcalfe, C. Petit, G. Puxty, J. Reimer, D.M. Reiner, E.S. Rubin, S.A. Scott, N. Shah, B. Smit, J.P.M. Trusler, P. Webley, J. Wilcox, N. Mac Dowell, Energy Environ. Sci. 11 (2018) 1062–1176.
[3] L. Deng, H. Kvamsdal, Green Energy Environ. 1 (2016) 179.
[4] S.E. Kentish, Ind. Eng. Chem. Res. 58 (2019) 12868–12875.
[5] J. Wang, J. Luo, S. Feng, H. Li, Y. Wan, X. Zhang, Green Energy Environ. 1 (2016) 43–61.
[6] Z.D. Dai, S. Fabio, N.G. Marino, C. Riccardo, L.Y. Deng, Int. J. Greenhouse Gas Control 86 (2019) 191–200.
[7] P. Bernardo, E. Drioli, G. Golemme, Ind. Eng. Chem. Res. 48 (2009) 4638–4663.
[8] L.M. Robeson, J. Membr. Sci. 320 (2008) 390–400.
[9] L.Y. Deng, T.J. Kim, M.B. Hägg, J. Membr. Sci. 340 (2009) 154–163.
[10] L.Y. Deng, M.B. Hägg, Int. J. Greenhouse Gas Control 26 (2014) 127–134.
[11] O.H. Leblanc, W.J. Ward, S.L. Matson, S.G. Kimura, J. Membr. Sci. 6 (1980) 339–343.
[12] G.J. Francisco, A. Chakma, X. Feng, J. Membr. Sci. 303 (2007) 54–63.
[13] Ho W S W. Membranes comprising salts of aminoacids in hydrophilic polymers: U.S. Patent 5,611,843[P]. 1997-3-18.
[14] Z.D. Dai, J. Deng, L. Ansaloni, S. Janakiram, L.Y. Deng, J. Membr. Sci. 578 (2019) 61–68.
[15] T.-J. Kim, B. Li, M.-B. Hägg, J. Polym. Sci., Part B Polym. Phys. 42 (2004) 4326–4336.
[16] Ho W S W. Membranes comprising aminoacid salts in polyamine polymers and blends: U.S. Patent 6,099,621[P]. 2000-8-8.
[17] Y. Cai, Z. Wang, C. Yi, Y. Bai, J. Wang, S. Wang, J. Membr. Sci. 310 (2008) 184–196.
[18] H. Matsuyama, A. Terada, T. Nakagawara, Y. Kitamura, M. Teramoto, J. Membr. Sci. 163 (1999) 221–227.
[19] M. Saeed, L.Y. Deng, J. Membr. Sci. 494 (2015) 196–204.
[20] M. Saeed, S. Rafiq, L.H. Bergersen, L.Y. Deng, Sep. Purif. Technol. 179 (2017) 550–560.
[21] L. Ansaloni, Y.N. Zhao, B.T. Jung, K. Ramasubramanian, M.G. Baschetti, W.S.W. Ho, J. Membr. Sci. 490 (2015) 18–28.
[22] A. Mondal, B. Mandal, J. Membr. Sci. 460 (2014) 126–138.
[23] C. Yi, Z. Wang, M. Li, J. Wang, S. Wang, Desalination 193 (2006) 90–96.
[24] Y.F. Li, Q.P. Xin, H. Wu, R.L. Guo, Z.Z. Tian, Y. Liu, S.F. Wang, G.W. He, F.S. Pan, Z.Y. Jiang, Energy Environ. Sci. 7 (2014) 1489–1499.
[25] R.W. Baker, B.T. Low, Macromolecules 47 (2014) 6999–7013.
[26] S. Mallakpour, V. Behranvand, in: V.K. Thakur, M.K. Thakur, R.K. Gupta (Eds.), Hybrid Polymer Composite Materials, Woodhead Publishing, 2017, pp. 263–289.
[27] M. Hayama, K.-I. Yamamoto, F. Kohori, K. Sakai, J. Membr. Sci. 234 (2004) 41–49.
[28] N. Bolong, A.F. Ismail, M.R. Salim, in: Sustainable Membrane Technology for Energy, Water, and Environment, John Wiley & Sons Inc., New Jersey, 2012, pp. 1–10.
[29] V.G. Kadajji, G.V. Betageri, Polymers 3 (2011) 1972–2009.
[30] J. Suh, H.J. Paik, B.K. Hwang, Bioorg. Chem. 22 (1994) 318–327.
[31] Z.D. Dai, L. Ansaloni, D.L. Gin, R.D. Noble, L.Y. Deng, J. Membr. Sci. 523 (2017) 551–560.
[32] M. Mulder, Basic Principles of Membrane Technology, second ed., Kluwer, Dordrecht, 1996.
[33] Z. Dai, L. Ansaloni, L. Deng, Green Energy Environ. 1 (2016) 102–128.
[34] Z.-H. Ping, Q.T. Nguyen, J. Néel, Macromol. Chem. Phys. 190 (1989) 437–448.
[35] A. El-Hag Ali, H.A. Shawky, H.A. Abd El Rehim, E.A. Hegazy, Eur. Polym. J. 39 (2003) 2337–2344.
[36] S.N. Cassu, M.I. Felisberti, Polymer 38 (1997) 3907–3911.
[37] Y.Y. Tan, G. Challa, Polymer 17 (1976) 739–740.
[38] D.T. Turner, A. Schwartz, Polymer 26 (1985) 757–762.
[39] L.Y. Deng, M.B. Hagg, J. Membr. Sci. 363 (2010) 295–301.
[40] M. Saeed, L.Y. Deng, Int. J. Greenhouse Gas Control 53 (2016) 254–262.
[41] X. Zhang, K. Takegoshi, K. Hikichi, Polymer 33 (1992) 712–717.
[42] Z. Dai, J. Deng, Q. Yu, R.M.L. Helberg, S. Janakiram, L. Ansaloni, L. Deng, ACS Appl. Mater Interf 11 (2019) 10874–10882.
[43] G.N. Hemantha Kumar, J. Lakshmana Rao, N.O. Gopal, K.V. Narasimhulu, R.P.S. Chakradhar, A. Varada Rajulu, Polymer 45 (2004) 5407–5415.
[44] S.H. Wen, F.Y. Zheng, M.W. Shen, X.Y. Shi, J. Appl. Polym. Sci. 128 (2013) 3807–3813.
[45] P. Srinivasa Rao, B. Smitha, S. Sridhar, A. Krishnaiah, Sep. Purif. Technol. 48 (2006) 244–254.
[46] J.N. Shen, C.C. Yu, G.N. Zeng, B. Van Der Bruggen, Int. J. Mol. Sci. 14 (2013) 3621–3638.
[47] S. Ben Hamouda, Q.T. Nguyen, D. Langevin, S. Roudesli, C. R. Chim. 13 (2010) 372–379.
[48] M.S.A. Rahaman, L. Zhang, L.-H. Cheng, X.-H. Xu, H.-L. Chen, RSC Adv. 2 (2012) 9165–9172.

Please cite this article as: R.M. Lilleby Helberg et al., PVA/PVP blend polymer matrix for hosting carriers in facilitated transport membranes: Synergistic enhancement of CO_2 separation performance, Green Energy & Environment, https://doi.org/10.1016/j.gee.2019.10.001